DISCRETE ELEMENT METHOD SIMULATION OF FORCE DISTRIBUTION ON THE COVERING DEVICE OF A TREE PLANTING MACHINE

SIMULAREA DISTRIBUȚIEI FORȚEI, UTILIZÂND METODA ELEMENTELOR DISCRETE, ASUPRA DISPOZITIVULUI DE ACOPERIRE AL UNEI MAȘINI DE PLANTAT POMI

Alin-Nicolae HARABAGIU*1), Dragoș-Nicolae DUMITRU*1), Vasilica ȘTEFAN¹1), Radu CIUPERCĂ¹1, Gabriel-Valentin GHEORGHE¹1), Melania Elena CISMARU¹1

(1)The National Institute of Research-Development for Machines and Installations Designed for Agriculture and Food Industry-INMA

Bucharest, Ion Ionescu de la Brad - 6, Sector 1, Bucharest, 013813 Romania

E-mail: alinhara04@gmail.com

DOI: https://doi.org/10.35633/inmateh-77-50

Keywords: tree planting machine, covering device, force distribution, soil moisture effect, DEM

ABSTRACT

This study uses discrete element method (DEM) simulations to examine how soil type, moisture content, and working speed affect forces on a tree planting machine's covering paddle, this method was applied to mimic real-world conditions and optimize working parameters. Maximum paddle forces increased from 263 N to 589 N across soil types and moisture contents, with higher water content and faster speeds increasing loads, especially in sandy soils. For example, in sandy soil, increasing moisture from 0% to 50% raised forces from 276 N to 392 N at 1 km/h and from 300 N to 589 N at 3 km/h. Clay soils showed generally lower forces (263–445 N). All measured forces remained within design limits, the objective was to establish a quantitative relation between soil moisture, working speed, and paddle reaction forces, highlighting their importance to ensure consistent seedling placement, minimize wear, and enhance equipment longevity.

REZUMAT

Acest studiu utilizează simulări prin metoda elementelor discrete (DEM) pentru a analiza modul în care tipul de sol, conținutul de apă și viteza de lucru influențează forțele asupra paletelor de acoperire ale unui echipament de plantat pomi, această metodă a fost aplicată pentru a imita condițiile din lumea reală și pentru a optimiza parametrii de funcționare. Forțele maxime măsurate au crescut de la 263 N la 589 N pe diferite tipuri de sol si umidități, crescând odată cu umiditatea solului și viteza de lucru, mai ales în solurile nisipoase. De exemplu, în sol nisipos, creșterea umidității de la 0% la 50% a ridicat forțele de la 276 N la 392 N la 1 km/h și de la 300 N la 589 N la 3 km/h. Solurile argiloase au prezentat forțe mai mici (263–445 N). Toate forțele măsurate s-au menținut în limitele de proiectare; obiectivul a fost stabilirea unei relații cantitative între umiditatea solului, viteza de lucru și forțele de reacție ale paletelor, evidențiind importanța acestora pentru a asigura o așezare uniformă a răsadurilor, a reduce uzura și a crește durabilitatea echipamentului.

INTRODUCTION

Mechanized tree planting plays a vital role in reforestation, sustainable agriculture, and land restoration worldwide (*Ersson et al., 2018*). Achieving precise tree seedling placement with minimal soil disturbance has become increasingly important, as it directly affects seedling survival, early root development, and long-term productivity. Soil covering devices are a key component in this process, influencing not only the positioning of seedlings but also moisture retention, weed suppression, and protection against environmental stressors (*Lu et al., 2024; Kemppainen et al., 2025*). Optimizing the performance of these machines can therefore significantly enhance both planting efficiency and seedling survival rates.

Recent advancements in agricultural machinery highlight the potential of simulation-based methods to reduce the time and cost associated with optimization through testing. Wu et al. (2024), for example, used simulations to develop and test an optimized soil covering device for a tree planting machine (Fig. 1), demonstrating measurable improvements in covering efficiency and tree seedling positioning. Similarly, Geng et al., 2022, optimized soil-covering systems for corn no-till planters, while Pan et al., 2023, presented a tobacco transplanting device that integrates digging and seedling placement through refined coordination between mechanical components and soil dynamics. These studies collectively show that the design of soil-interacting components significantly affects seedling placement, initial rooting, and the surrounding soil environment necessary for early growth.



Fig. 1 - Field experiments for a soil covering device (Wu et al., 2024)

The Discrete Element Method (DEM) has emerged as a particularly valuable tool for investigating soil—tool interactions at the particle level. Three-dimensional DEM models offer a more accurate representation of soil particle behavior compared to two-dimensional approaches (*Ucgul et al., 2014*). *Ucgul et al.* further demonstrated that appropriate contact models and simulation parameters for cohesionless soils can capture realistic particle flow and force distributions, while extensions to cohesive and adhesive soil properties allow the modelling of a wider range of real-world conditions. DEM simulations have been successfully applied to soil-tillage and furrow-opening processes (*Tamás et al., 2013; Fang et al., 2016; Li et al., 2023; Aikins et al., 2023*), providing insight into how individual soil particles respond to mechanical forces (Fig. 2). *Makange et al., 2021*, illustrated that combining DEM simulations with analytical methods can reliably predict subsoiling performance. These studies collectively underscore the reliability of DEM in reproducing realistic soil behavior and force distributions, making it an indispensable tool for designing and optimizing planting machinery, although DEM has been widely used for tillage and furrow openers, only few studies investigated force transmission to planting mechanisms during soil covering.

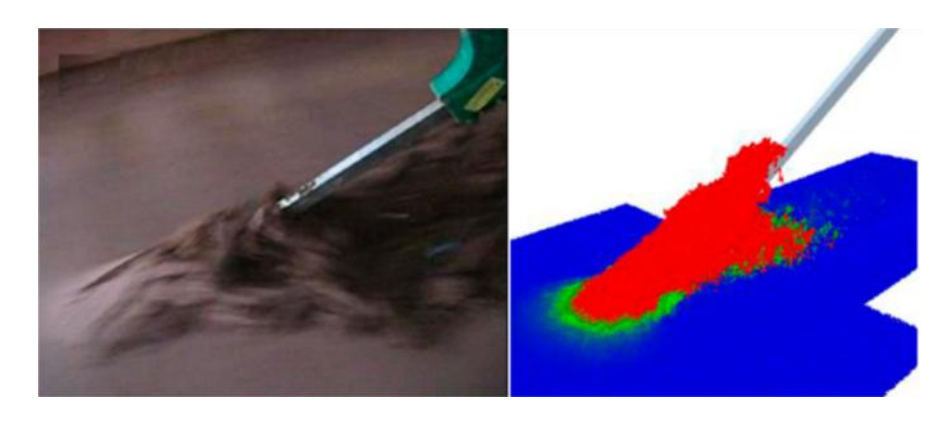


Fig. 2 - Discrete element method simulation of a narrow furrow opener (Aikins et al., 2023)

Complementing these simulation studies is the experimental work of *Liyan Li et al., 2020*, which provided a detailed simulation analysis of the soil covering process. Their research validated the DEM approach by comparing computational predictions with practical tests, establishing a clear relation between simulation outcomes and real-world behavior.

Recent reviews by *Mwiti et al., 2023 and Wang et al., 2023*, on how tools interact with soil (Fig. 3) and how soil breaks apart under mechanical force, remind us that soil doesn't behave in a simple, predictable way, it's affected by many different factors. Finite element studies, like those by *Hashaam et al., 2023*, offer useful insights, but they also show that traditional models struggle to accurately represent how loose, granular materials like soil really behave.

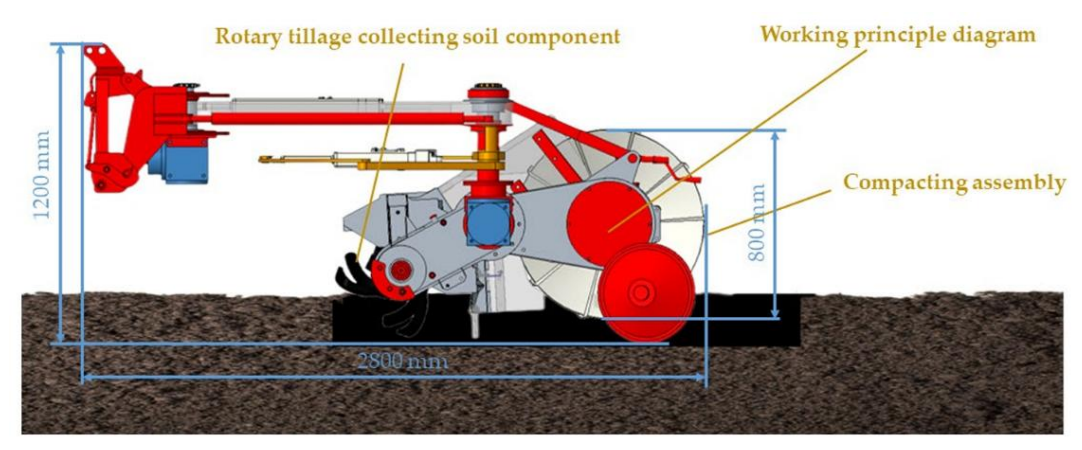


Fig. 3 - Ridge device in a paddy field

Building on these insights, the main objective of this research is to evaluate the dynamics of soil interacting with the covering device of a tree planting machine using DEM-based simulations. The study focuses on quantifying the forces applied to the soil covering mechanism and understanding how these forces are transmitted to the planting arm. It was specifically decided to use DEM simulations rather than basic finite element method (FEM) simulations in order to create a more realistic representation of soil behavior and operating conditions, closely mirroring real-world experiments. By integrating detailed simulations, the research aims to analyze the impact of soil moisture content and working speed on the tree planting accuracy, ultimately providing guidelines for improving tree planting efficiency, reducing mechanical stress on planting equipment, and ensuring precise tree seedling placement under various soil types.

MATERIALS AND METHODS

The tree planting machine design

This study focuses on a tree planting machine (Fig. 4) consisting of several key components, including the furrow opener (1), soil covering mechanism (2), tree seedling planting system (3), worker's seats (4) and storage boxes for the seedlings (5). The primary function of the machine is to prepare the soil and ensure proper coverage over the seedling after planting. The machine performs trenching and soil covering operations simultaneously, unlike traditional systems that use separate machines for each process. Once the trenching operation is complete and the seedlings are placed, the left and right soil covering wheels simultaneously dig and loosen the soil while moving the material into the planting trench, effectively covering the tree seedlings with soil in one continuous motion.

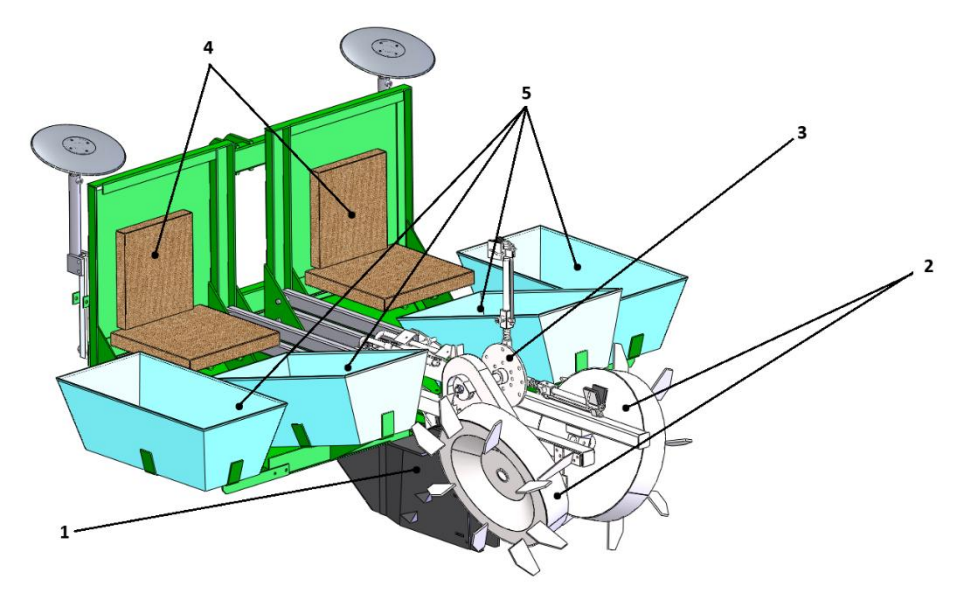


Fig. 4 - The 3D model of the tree planting machine

1 - furrow opener; 2 - soil covering mechanism; 3 - tree seedling planting system; 4 - worker's seats; 5 - storage boxes

The machine used for this simulation is designed to operate under typical field conditions, with the following specifications:

Machine width: 2.6 mSpeed: 1 to 3 km/hWorking depth: 0.3 m

• Weight: 850 kg (approximate, varies with load)

• Furrow opener: V-shaped

Soil covering wheels diameter: 0.6 m

Number of paddles: 8

The working principle of the tree planting machine's soil covering device is as follows. The soil covering device is mounted at the rear end of the frame, on both the left and right sides. The soil covering wheels on each side are arranged in a 'V' shape at a 40° angle relative to each other, they are equipped with paddles to help dislocate compacted soil. The seedling pickup mechanism works through a simple mechanical system. As the arm moves along its path, it interacts with a profiled cam. When the arm reaches the cam, it gradually compresses a spring until it's fully loaded, which causes the gripping jaws to close. This design makes sure the seedling is held right, using just the movement of the mechanism and the spring's stored energy, no extra power needed.

In order for this motion to occur, the force transferred to the planting arm must overcome the spring force, this force is directly influenced by the reaction force exerted on the paddles. If the soil's resistance is insufficient, the spring won't compress fully, preventing the gripping jaws from closing properly and the system from picking up the seedlings. Because the interaction between the paddles and soil is complex and depends on various factors like soil type and moisture, it's essential to simulate and accurately measure the forces acting on the paddles. This simulation helps ensure the mechanism is properly designed to function reliably under different working conditions.

The simulation setup

To develop accurate particle and geometric interactions, previous EDEM simulation studies on tree planting machinery and soil moisture content (*Li et al., 2021; Li et al., 2022; Zhou et al., 2025*) were reviewed and used as references. For the best accuracy, it is essential to define the soil parameters, the material properties of the components interacting with the soil, and the contact parameters between them. Contact parameters such as the coefficient of restitution, coefficient of static friction, and coefficient of rolling friction are key factors in simulating the effect of moisture, these properties were chosen based on findings from previous researches (*Chen et al., 2022; Luding, 2008; Gilabert et al., 2007*). All these properties are summarized in Table 1.

Different soil types properties

Table 1

Soil type	Moisture content (%)	Poisson ratio	Density (kg/m³)	Shear modulus (MPa)	Restitution coefficient	Static friction coefficient	Rolling friction coefficient
Sandy	0	0.25	2670	30	0.80	0.92	0.06
	25	0.26	2799	33	0.69	1.17	0.12
	50	0.28	2928	33	0.55	1.42	0.21
Clay	0	0.38	1245	10	0.66	0.67	0.08
	25	0.40	1250	10	0.57	0.85	0.15
	50	0.43	1308	10	0.45	1.03	0.26

For this study two soil beds were created and used, each with different properties in order to replicate real-world conditions, one with sandy soil and the other with clay soil, these properties were modified to simulate three different moisture contents as well. The average radius of the sandy soil particles was set to 10 mm, based on values reported in previous studies. A Hertz-Mindlin (no-slip) contact model was used to describe interactions both between soil particles and with the machine surfaces. This model is appropriate for sandy soil due to its low inter-particle friction and limited adhesion, allowing the Hertz-Mindlin formulation to accurately capture its contact behavior. For the clay soil, however, a different model was required due to its cohesive and plastic properties. Therefore, the Edinburgh Elasto-Plastic Adhesion (EEPA) contact model was

applied. The EEPA model includes a nonlinear hysteretic spring to represent elastic-plastic contact deformation and an adhesive force term that varies with the extent of plastic deformation, making it suitable for simulating cohesive clay behavior. The EEPA offers a versatility that allows it to be used in both linear and non-linear modes. When two particles or agglomerates are pressed together, they undergo elastic and plastic deformations. It is assumed that the pull-off strength (adhesion) increases with an increase of the plastic contact area, prior studies were reviewed to determine the appropriate contact parameters for this contact model (*Thakur et al., 2014*), which were then implemented within EDEM to ensure accurate simulation results. The contact force-displacement relationship for microscopic particles is shown in the figure 5.

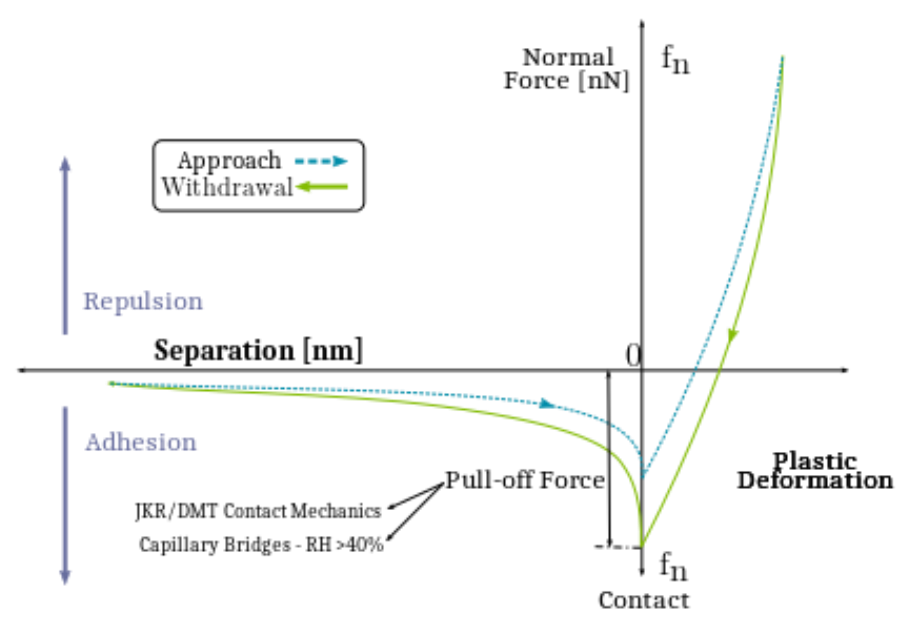


Fig. 5 – Schematic illustration of observed force-separation curves for adhesive particles

Lastly, the soil bed with 5000 mm length, 2000 mm width, and 1000 mm height was generated within EDEM to be used for our simulations, this domain size allowed for a better soil compaction, an even force distribution and a more realistic simulation environment. To reduce simulation calculation time—without compromising the accuracy of the results—parts that do not interact with the soil and do not influence the soil's reaction forces were removed. The resulting three-dimensional model was then imported into EDEM (Fig. 6 a). The simulations were conducted at forward speeds of 1 and 3 km/h, to reflect realistic operating conditions, a linear motion was applied to simulate the machine moving through the soil, the reaction forces were obtained from the EDEM simulation using the manual selection tool, (Fig. 6 b) in order to select the face of the paddle at its maximum working depth, where the highest loads occur. The resulted data was then evaluated using EDEM's built-in Analyst tool.

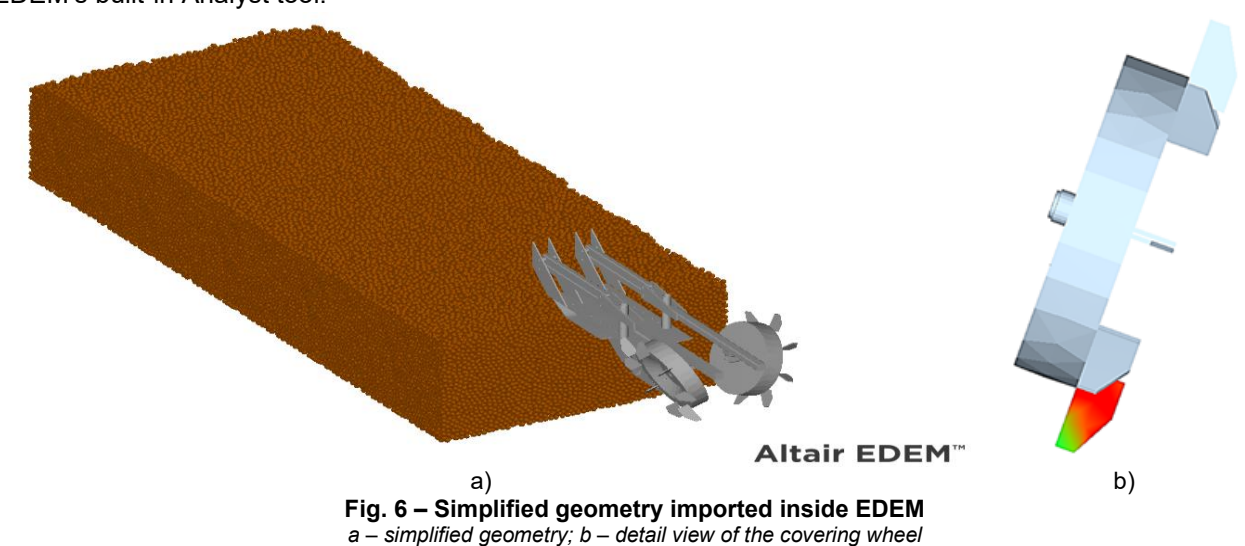


Figure 7 illustrates the transmission mechanism that drives the planting arm. The load applied to the paddle of the soil-covering wheel (1) is transmitted through a series of three toothed wheels: the first wheel is directly connected to the covering device (2), the second wheel serves as an intermediary gear (3), and the third wheel is linked to the planting mechanism (4). This transmission configuration enables smooth movement of the planting arm mechanism (5). Using the reaction force acting on the paddle (obtained from EDEM simulations), along with the known gear diameters (180 mm, 180 mm, and 220 mm) and the distance from the center of the third toothed wheel to the planting-arm actuation point (130 mm), the transmitted torque can be determined. The measured moments of inertia (M₁, M₂ and M₃) of the transmission components are key parameters for estimating the magnitude of force delivered to the planting arm. This transmitted force is critical for ensuring reliable seedling placement. If the force is too low, the seedlings may slip from the gripper, resulting in uneven spacing and improper positioning, which can reduce survival rates. If the force is too high, excessive vibration may occur, accelerating mechanical wear or causing damage to the seedlings due to overly firm gripping, thus compromising seedling viability.

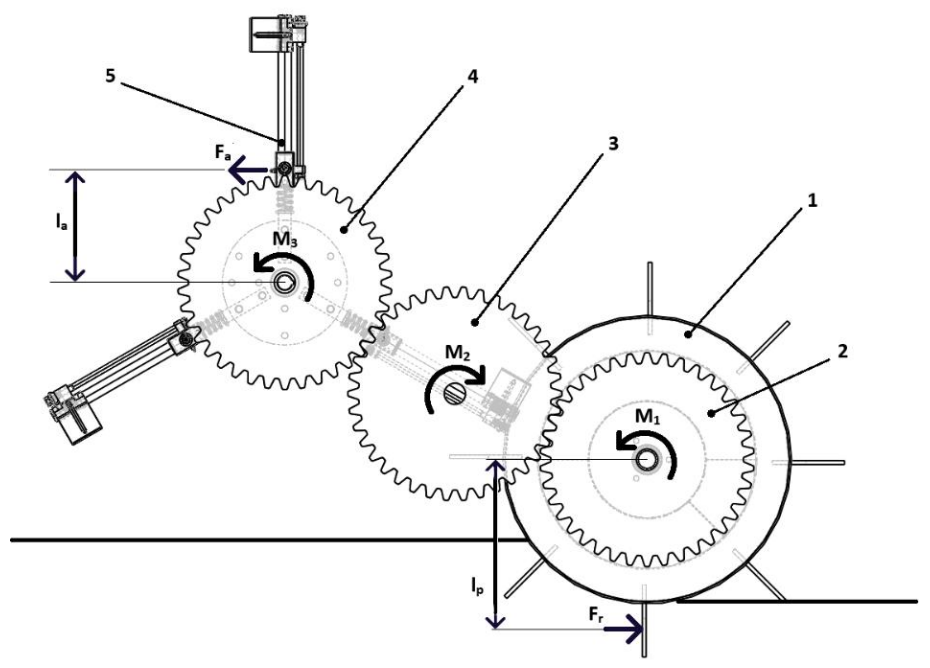


Fig. 7 - Tree planting machine transmission diagram

1 – soil-covering wheel; 2 – first toothed-wheel; 3 – second toothed-wheel; 4 – third toothed-wheel; 5 – planting arm.

According to Filipoiu and Tudor (2006), under working-load conditions, the soil reaction force F_r generates the moment M_I on the first toothed-wheel of the transmission. This moment is transmitted to the intermediary wheel producing a moment of inertia M_2 , and finally to the last wheel, where the moment M_3 is generated, this moment influences the movement of the planting arm mechanism, these moments and forces can be determined using the following formulas:

$$M_1 = F_r \cdot l_p \text{ [N m]} \tag{1}$$

$$\frac{M_2}{M} = \frac{D_2}{D} \tag{2}$$

$$M_{1} = F_{r} \cdot l_{p} \text{ [N m]}$$

$$\frac{M_{2}}{M_{1}} = \frac{D_{2}}{D_{1}}$$

$$\frac{M_{3}}{M_{2}} = \frac{D_{3}}{D_{2}}$$

$$M_{3} = F_{a} \cdot l_{a} \text{ [N m]}$$

$$e \text{ first teathed wheel (N m)}$$

$$(4)$$

$$M_3 = F_a \cdot l_a \text{ [N m]} \tag{4}$$

where: M_l is the moment of inertia on the first toothed-wheel (N m);

 l_p – length from the first gear to the paddle (m);

 F_r – soil resistance force acting on the paddle (N);

 M_2 – second toothed-wheel moment of inertia (N m);

 D_2 – second toothed-wheel diameter (m);

 D_I – first toothed-wheel diameter (m);

 M_3 – third toothed-wheel moment of inertia (N m);

 D_3 – third toothed-wheel diameter (m);

 F_a – force acting on the planting arm (N);

 l_a – length from the third gear center to the arm action system (m).

Using all of this information the resulting force acting on the planting arm must exceed the opposing forces generated by the two torsion springs, DIN 2194:2002, and one compression spring, DIN EN 15800:2009, located within the arm mechanism, the measured force to compress all these springs and fully close the gripping mechanism was around 160 N.

This force represents a key parameter in evaluating whether the generated force is enough to fully close the gripping mechanism responsible for securing the tree seedlings during planting. The objective of the present study is to establish the optimal operating parameters for the tree planting machine in order to ensure reliable mechanism performance and consistent planting quality.

RESULTS

This study determined the reaction force exerted by soil on a paddle and evaluated how soil type, moisture content, and forward working speed influence that force. To do this, two soil types (sand and clay), three moisture levels (0–50%), and two working speeds (1 and 3 km/h) were tested, to examine their individual and combined effects.

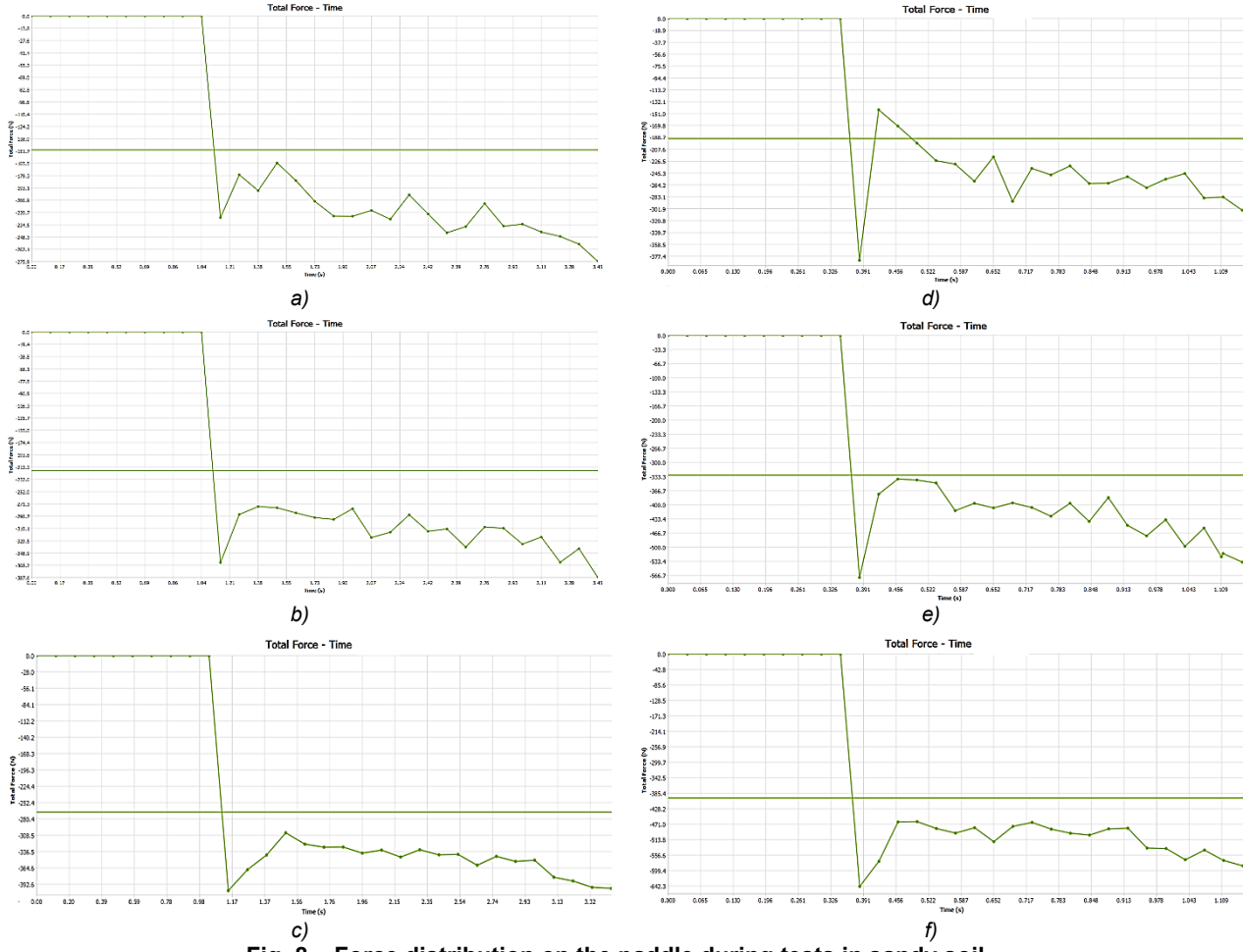
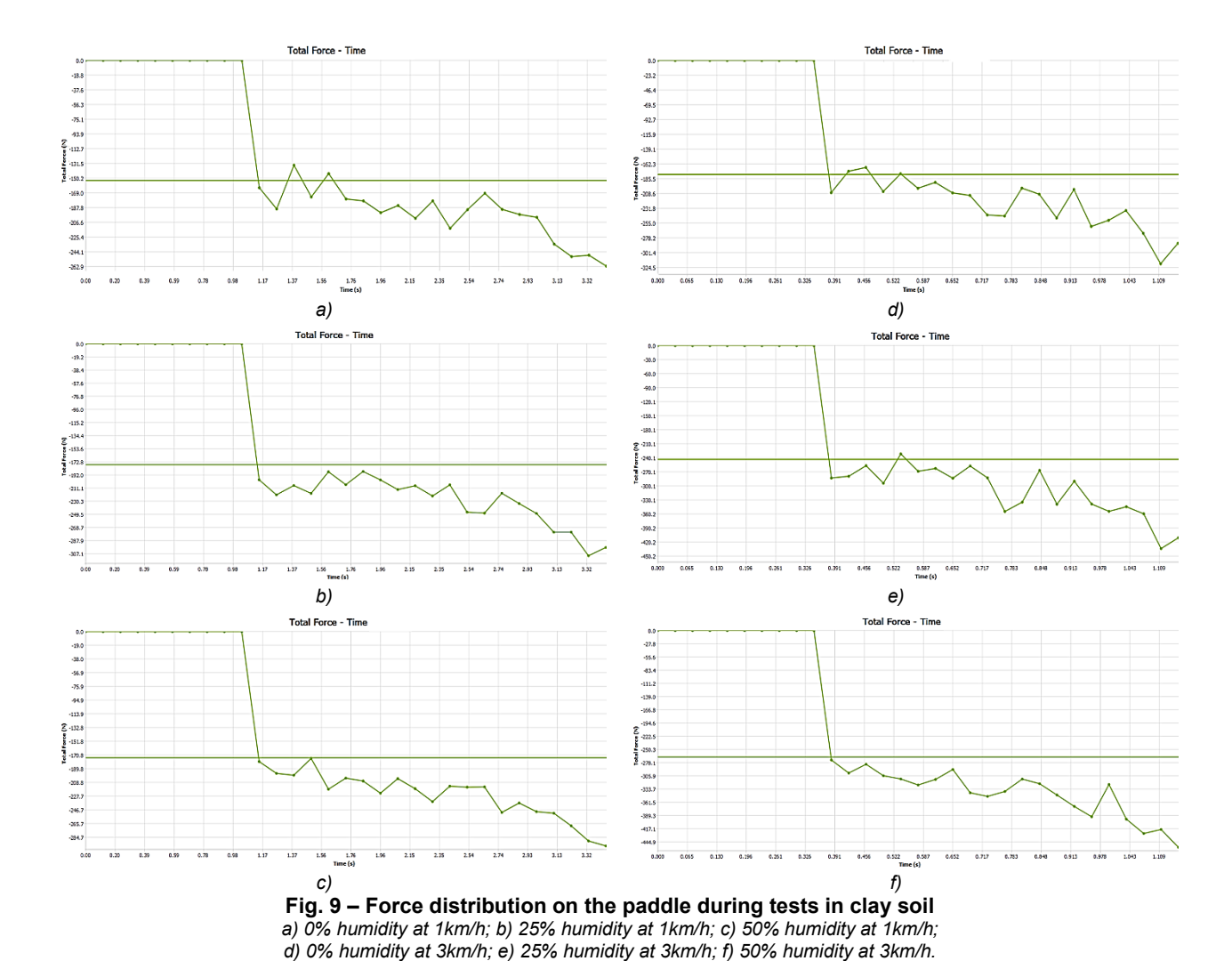


Fig. 8 – Force distribution on the paddle during tests in sandy soil a) 0% humidity at 1km/h; b) 25% humidity at 1km/h; c) 50% humidity at 1km/h; d) 0% humidity at 3km/h; e) 25% humidity at 3km/h; f) 50% humidity at 3km/h.

The simulations conducted on sandy soil revealed a high force spike upon entering the soil regardless of the working speed, with more abrupt spikes on dry sand. The water content increase showed a directly proportional increase in the force applied to the paddle, specifically, simulations on dry sand resulted in a peak force of approximately 300 N (Fig. 8-a, d), while the wet sand almost doubled this value, peaking at around 589 N (Fig. 8-c, f). The mean force values also reflected this trend, going from 155 N in dry conditions to 385 N in wet conditions. These results highlight the important role of water content in maintaining stable operation in sandy soils. Simulations with higher water content not only showed more stable loadings but also significantly reduced the initial force spike experienced when the paddle entered the soil.



The lower-speed tests, (Fig. 9 – a, b, c), showed a steady force profile across all moisture levels. The total reaction force showed a mean value between around 150 N and 170 N, with only slight differences in peak forces as moisture increased from 0 % to 50 %. Specifically, the driest clay soil peaked near 263 N, while the wettest soil reached about 285 N. These results indicate that, at slow speeds, the humidity levels only slightly raise the soil resistance and does not introduce abrupt force spikes, the paddle-soil contact remaining uniform regardless of water content. On the other hand, when the forward speed was raised, (Fig. 9 – d, e, f), the interaction became stronger and more variable. Across the same three moisture levels, peak reaction forces now ranged from approximately 324 N (dry clay soil) to 445 N (wet clay soil)—around a 50% increase compared to the 1 km/h tests. Not only the peaks were higher, but the force curves also displayed greater fluctuation in the wetter conditions, with 25 % and 50 % tests showing noticeable oscillations. This emphasizes that, at higher velocities, wetter clay produces sharper loading on the paddle.

These findings show a clear interaction between the working speed and soil moisture levels. At lower speeds, increasing moisture content has only a small effect on resistance, while at higher speeds it amplifies the magnitude and variability of the reaction force. This suggests that operations involving fast paddle motion in wet clay soil will encounter higher loads but also more noticeable force spikes, conditions that could accelerate wear or lead to mechanical failure. Previous formulas were applied in order to measure the transferred force to the action mechanism of the tree planting arm, all the results are showed in Table 2.

Measured force on the paddle and the transferred force results

Working speed Water level content Max force on the paddle Max transferred force Soil type (km/h) (%)(N) (N) Sandy soil 1 0 276 225 1 25 387 315 Sandy soil 1 50 392 319 Sandy soil 3 0 245 Sandy soil 300

Table 2

Soil type	Working speed (km/h)	Water level content (%)	Max force on the paddle (N)	Max transferred force (N)
Sandy soil	3	25	530	432
Sandy soil	3	50	589	458
Clay soil	1	0	263	212
Clay soil	1	25	307	235
Clay soil	1	50	285	240
Clay soil	3	0	324	264
Clay soil	3	25	420	342
Clay soil	3	50	445	363

The analysis of the measured forces indicates that soil type, working speed, and soil moisture content all play a critical role in the performance of the seedling planting machine. In sandy soil, low moisture levels at low working speeds (1 km/h) result in transferred forces of 225-245 N, which are safely above the critical minimum of 160 N required to prevent seedling slippage. As soil moisture increases, transferred forces rise significantly, reaching up to 458 N at 3 km/h and 50% moisture, a level that poses a risk of over-compressing the gripping mechanism and potentially damaging the seedlings. In clay soil, forces are generally lower, with low-speed, low-moisture conditions (1 km/h, 0-25% moisture) producing transferred forces of 212-235 N, which approach the threshold for slippage and may result in uneven seedling placement, compromising survival. Higher working speeds and moisture in clay soil (3 km/h, 25-50% moisture) yield transferred forces in the range of 342-363 N, providing a sufficient margin to ensure secure gripping without excessive risk of damage. Overall, the optimal planting conditions appear to occur at low speeds and moderate moisture levels, where transferred forces are well above the minimum required to prevent slippage but below levels that could cause mechanical over-compression. Conversely, the most unfavorable conditions are associated with either low transferred forces, which increase the likelihood of seedling slippage and uneven planting, or excessively high forces, which may physically damage the seedlings. These findings highlight the importance of carefully adjusting operating parameters to balance reliable mechanism performance with the protection of seedlings during planting.

To examine the effects of soil type, working speed, and water content on maximum transferred force, a one-way ANOVA was performed for each factor individually. Descriptive statistics, including mean and standard deviation, were calculated to summarize the central tendency and variability of the force measurements. The ANOVA F-values and corresponding p-values provide statistical evidence regarding whether differences between factor levels are significant. This approach enables a clear evaluation of the relative influence of each factor on transferred force, highlighting which operational or environmental conditions contribute most to variations in mechanical load (Table 3).

Descriptive statistics results for maximum transferred force

Table 3

Factor	Mean (N)	Std Dev (N)	F-value	p-value
Soil type	304.17	78.56	1.48	0.252
Working speed	304.17	66.52	5.40	0.043
Water content	304.17	64.98	4.67	0.056

The p-value indicates the probability that the observed differences between groups occurred by random chance. A p-value<0.05 is considered statistically significant.

The results indicate that working speed has a statistically significant effect on maximum transferred force, as evidenced by the F-value of 5.40 and p-value below 0.05. While soil type and water content show trends toward higher forces, their effects are not statistically significant at the 5% level, although water content approaches significance. Overall, these findings suggest that operational factors, particularly speed, play a more critical role than environmental factors, such as soil type or moisture content in determining the mechanical load transferred, providing guidance for optimizing soil-engaging mechanisms under varying field conditions. Based on these findings it is recommended that the tree planting machine can be safely used on both sandy and clay soil, as soil types does not significantly affect transferred force. However, water content should be carefully monitored, since higher moisture levels can increase the gripping strength and potentially damage the plant. In addition, higher working speeds are not advised, as they generate excessive forces that may lead to mechanical stress, structural failure, or seedling injury. By maintaining moderate speeds and controlling soil moisture, the tree planting machine can operate with a smooth and consistent flow, ensuring improved planting accuracy and reliability in the field.

CONCLUSIONS

These results indicate that the maximum force acting on the paddle is strongly dependent on both working speed and soil water content. For both sandy and clay soils, maximum paddle force increases with moisture. At 1 km/h the increase is moderate and tends to stabilize above approximately 25% water content. Even at lower speeds, sandy soil consistently requires higher forces than clay across the tested moisture levels.

The influence of moisture becomes markedly more pronounced at 3 km/h: maximum forces rise sharply with increasing water content, particularly in sandy soil, where the force nearly doubles as moisture increases. Clay soil also shows a clear increase with moisture, albeit less abrupt than in the sandy case. In short, higher working speeds combined with higher water contents produce substantially larger loads on the paddle—an effect that is most severe in sandy soils—and must be taken into account when sizing powertrains and safety margins to avoid mechanical overload.

The relatively gradual increase in force observed under moderately wet soil conditions indicates stable tool—soil interaction, which contributes to uniform seedling placement. Based on these findings, lower forward speeds are recommended in wet soils, whereas moderate speeds are suitable in dry soils to maintain a steady planting motion, improve placement accuracy, and reduce transient overloads. These operating strategies are also expected to enhance energy efficiency and mechanical reliability, provided that the transmission and drive components are designed to accommodate the corresponding load ranges.

Finally, because there are no prior studies that comprehensively address this particular tool—soil/transmission interaction, the present simulation dataset establishes a baseline for the phenomenon. To strengthen and validate these findings, the simulated results will be compared with experimental field tests measurements in follow-up work. This experimental validation will support more confident extrapolation of the results to design and operational recommendations.

Finally, as no prior studies have comprehensively examined this specific tool—soil and transmission interaction, the present simulation results serve as an initial reference dataset for the phenomenon. To further strengthen and validate these findings, the simulated outcomes will be compared with measurements obtained from subsequent field experiments. Such experimental validation will allow more confident extrapolation of the results toward design guidelines and operational recommendations.

ACKNOWLEDGEMENT

This work was supported by a project of the Ministry of Research, Innovation and Digitization, through Program NUCLEU - Project: PN 23 04 01 05 - Innovative technology for the maintenance of fruit plantations, contract no. 9N/ 01.01.2023.

REFERENCES

- [1] Aikins K. A., Ucgul M., Barr J. B., Awuah E., Antille D. L., Jensen T. A., Desbiolles J. M. A. (2023). Review of discrete element method simulations of soil tillage and furrow opening. *Agriculture*., 13:541, https://doi.org/10.3390/agriculture13030541
- [2] Chen B., Liu Y., Yu Q., Chen X., Miao Y., He Y., Chen J., Zhang J. (2022). Calibration of soil discrete element contact parameter in rhizome medicinal materials planting area in hilly region. *INMATEH Agric Eng.*, 68:51, https://doi.org/10.35633/inmateh-68-51
- [3] Deutsches Institut für Normung e V. (2002). Cold coiled cylindrical helical torsion springs—requirements and testing. *DIN* 2194:2002.
- [4] Deutsches Institut für Normung e V. (2009). Springs—quality specifications for cold coiled compression springs. *DIN EN* 15800:2009-03.
- [5] Ersson B. T., Laine T., Saksa T. (2018). Mechanized tree planting in Sweden and Finland: current state and key factors for future growth. *Forests.*, 9:370, https://doi.org/10.3390/f9070370
- [6] Fang H., Ji C., Chandio F. A., Guo J., Zhang Q., Arslan C. (2016). Analysis of soil dynamic behavior during rotary tillage based on distinct element method. *Trans Chin Soc Agric Mach.*, 47:004, https://doi.org/10.6041/j.issn.1000-1298.2016.03.004
- [7] Filipoiu I. D., Tudor A. (2006). Proiectarea transmisiilor mecanice. Bren.
- [8] Geng Y., Wang X., Zhong X., Zhang X., Chen K., Wei Z., Lu Q., Cheng X., Wei M. (2022). Design and optimization of a soil-covering device for a corn no-till planter. *Agriculture*., 12:1218, https://doi.org/10.3390/agriculture12081218

- [9] Gilabert F. A., Roux J.-N., Castellanos A. (2007). Computer simulation of model cohesive powders: influence of assembling procedure and contact laws on low consolidation states. *Phys Rev E.*, 75:011303, https://doi.org/10.1103/PhysRevE.75.011303
- [10] Hashaam M., Akram M. W., Ahmad M., Akram M. Z., Faheem M., Maqsood M., Aleem M. (2023). 3D finite element analysis of tine cultivator and soil deformation. *Res Agric Eng.*, 69:107–117, https://doi.org/10.17221/58/2022-RAE
- [11] Kemppainen K., Kärhä K., Laitila J., Sairanen A., Kankaanhuhta V., Viiri H., Peltola H. (2025). Evaluation of the productivity and costs of excavator-based mechanized tree planting in Finland based on automated data collection. *Silva Fenn.*, 59:25004, https://doi.org/10.14214/sf.25004
- [12] Li J., Xie S., Liu F., Guo Y., Liu C., Shang Z., Zhao X. (2022). Calibration and testing of discrete element simulation parameters for sandy soils in potato growing areas. *Appl Sci.*, 12:10125, https://doi.org/10.3390/app121910125
- [13] Li L., Gong X., Xu T., Guo P. (2020). Simulation analysis of soil covering process. *J Phys Conf Ser.*, 1578:012099, https://doi.org/10.1088/1742-6596/1578/1/012099
- [14] Li S., Diao P., Zhao Y., Miao H., Li X., Zhao H. (2023). Calibration of discrete element parameter of soil in high-speed tillage. *Res Agric Eng.*, 71(3), https://doi.org/10.35633/inmateh-71-21
- [15] Lu Q., Zhao J., Liu L., Liu Z., Wang C. (2024). Design and experiment of a soil-covering and-pressing device for planters. *Agriculture*., 14:1040, https://doi.org/10.3390/agriculture14071040
- [16] Luding S. (2008). Cohesive, frictional powders: contact models for tension. *Granular Matter.*, 10:235–246, https://doi.org/10.1007/s10035-008-0099-x
- [17] Makange N. R., Ji C., Nyalala I., Sunusi I. I., Opiyo S. (2021). Prediction of precise subsoiling based on analytical method, discrete element simulation and experimental data from soil bin. *Sci Rep.*, 11:11082, https://doi.org/10.1038/s41598-021-90682-w
- [18] Mwiti F., Gitau A., Mbuge D., Misiewicz P., Njoroge R., Godwin R. (2023). Mechanized tillage-induced compaction and its effect on maize (Zea mays L.) growth and yield a comprehensive review and analysis. *AMA Agric Mech Asia Afr Lat Am.*, 54:7, https://doi.org/10.2139/ssrn.4891677
- [19] Pan Z., Sun T., Wang X., Hou Q., Lv S., Zhang L., Yang Z., Zhang X. (2023). Design and optimization of an integrated excavation and transplanting device for tobacco. *INMATEH Agricultural Engineering*, 71(3), https://doi.org/10.35633/inmateh-71-34
- [20] Tamás K., Jóri T. J., Mouazen A. M. (2014). Modelling soil-sweep interaction with discrete element method. *Soil Tillage Res.*, 138:69–77, https://doi.org/10.1016/j.still.2013.09.001
- [21] Thakur S. C., Morrissey J. P., Sun J., Chen J. F., Ooi J. Y. (2014). Micromechanical analysis of cohesive granular materials using the discrete element method with an adhesive elasto-plastic contact model. *Granular Matter.*, 16:383–400, https://doi.org/10.1007/s10035-014-0506-4
- [22] Ucgul M., Fielke J. M., Saunders C. (2014). Three-dimensional discrete element modelling of tillage: determination of a suitable contact model and parameters for a cohesionless soil. *Biosyst Eng.*, 121:105–117, https://doi.org/10.1016/j.biosystemseng.2014.02.005
- [23] Ucgul M., Fielke J. M., Saunders C. (2014). Three-dimensional discrete element modelling (DEM) of tillage: accounting for soil cohesion and adhesion. *Biosyst Eng.*, 125:147–158, https://doi.org/10.1016/j.biosystemseng.2014.11.006
- [24] Wang J., Xiang Y., Wang C., Xu C., Zhu G., Gu Z., Wang J., Tang H. (2023). The method and experiment of kinetic determination for the rotary soil-engaging components of agricultural machinery using a compacting device in a paddy field as an example. *Agronomy*, 13(3), Article 775. https://doi.org/10.3390/agronomy13030775
- [25] Wu X., Jiang Z., Zhang L., Hu X., Li W. (2024). Optimization design and experimentation of a soil covering device for a tree planting machine. *Agriculture*, 14(3), Article 346. https://doi.org/10.3390/agriculture14030346
- [26] Zhou Y., Sun R., Zhang M., Hao Y. (2025). A study on the passing performance of a two-tire model of a special vehicle based on a loose road surface. J Phys Conf Ser., 2951:012051, https://doi.org/10.1088/1742-6596/2951/1/012051